

Specificity of Sites within Eight-Membered Ring Zeolite Channels for Carbonylation of Methyls to Acetyls

Aditya Bhan,[†] Ayman D. Allian,[†] Glenn J. Sunley,[‡] David J. Law,[‡] and Enrique Iglesia^{*†}

Contribution from the Department of Chemical Engineering, University of California at Berkeley, Berkeley, California 94720, and [‡]BP Chemicals Limited, Hull Research and Technology Center, Saltend, Hull HU 12 8DS, U.K.

Received January 10, 2007; E-mail: iglesias@berkeley.edu

Abstract: The acid-catalyzed formation of carbon–carbon bonds from C₁ precursors via CO insertion into chemisorbed methyl groups occurs selectively within eight-membered ring (8-MR) zeolite channels. This elementary step controls catalytic carbonylation rates of dimethyl ether (DME) to methyl acetate. The number of O–H groups within 8-MR channels was measured by rigorous deconvolution of the infrared bands for O–H groups in cation-exchanged and acid forms of mordenite (M,H-MOR) and ferrierite (H-FER) after adsorption of basic probe molecules of varying size. DME carbonylation rates are proportional to the number of O–H groups within 8-MR channels. Na⁺ cations selectively replaced protons within 8-MR channels and led to a disproportionate decrease in carbonylation turnover rates (per total H⁺). These conclusions are consistent with the low or undetectable rates of carbonylation on zeolites without 8-MR channels (H-BEA, H-FAU, H-MFI). Such specificity of methyl reactivity upon confinement within small channels appears to be unprecedented in catalysis by microporous solids, which typically select reactions by size exclusion of bulkier transition states.

Introduction

Carbonylation provides a convenient route to functionalize C₁ intermediates via formation of carbon–carbon bonds at low temperatures.^{1–3} Solid acid catalysts catalyze carbonylation of alkanols and ethers via Koch-type reactions, in which surface alkyl groups have been proposed to react with CO to form acylium ions, which form carboxylic acids upon subsequent hydrolysis.^{2,4–6} Carbonylation of methanol and DME on zeolites and polyoxometalate clusters occurs concurrently with extensive deactivation and hydrocarbon formation. We have recently reported the selective carbonylation of dimethyl ether (DME) to methyl acetate, a precursor to acetic acid, at low temperatures (400–460 K) on acidic zeolites, without detectable homologation reactions or catalyst deactivation.^{7,8} Kinetic and spectroscopic probes showed that carbonylation involves the initial formation of methyl groups via DME reactions with acidic OH groups and subsequent propagation reactions, in which methyl

groups (or oxonium-ion derivatives) react slowly with CO via insertion into the C–O bonds in bound methyls. The acetyls formed then react with DME in methoxylation reactions that regenerate methyl intermediates. Carbonylation rates (per total H⁺) were strongly influenced by the identity of the zeolite and the density of OH groups and were strongly inhibited by the presence of water. The basis for such marked effects of structure, site density, and water remained unclear at the time of our earlier reports.

Here, we present evidence for the unique reactivity of CH₃ groups located within eight-membered ring (MR) channels in mordenite (MOR) and ferrierite (FER) in carbonylation reactions. H⁺ groups (and the CH₃ groups formed via reactions of DME with H⁺) within 10-MR and 12-MR channels in H-MFI, H-BEA, and H-FAU gave undetectable carbonylation rates.^{7,8} We show here that these marked effects of zeolite structure and H⁺ density reflect the initial presence of H⁺ and the ultimate presence of CH₃ groups during DME-CO reactions, within 8-MR channels, and their higher reactivity compared with those within less constrained 10-MR, 12-MR, or mesoscopic channels for CO insertion reactions. These findings provide evidence of unprecedented clarity for transition state specificity and for the remarkable effects of spatial constraints in catalytic reactions within microporous solids.

Experimental Methods

Catalyst Synthesis. NH₄-MOR (Si/Al = 10, Zeolyst) and NH₄-FER (Si/Al = 33.5, Zeolyst) were treated in flowing dry air (zero grade, Praxair) at 773 K (0.0167 K s⁻¹) for 3 h to remove organic species

[†] Department of Chemical Engineering, University of California at Berkeley.

[‡] BP Chemicals Limited.

- (1) Bagno, A.; Bukala, J.; Olah, G. A. *J. Org. Chem.* **1990**, *55*, (14), 4284.
- (2) Stepanov, A. G.; Luzgin, M. V.; Romannikov, V. N.; Zamaraev, K. I. *J. Am. Chem. Soc.* **1995**, *117* (12), 3615.
- (3) Sunley, G. J.; Watson, D. J. *Catal. Today* **2000**, *58* (4), 293.
- (4) Wegman, R. W. *J. Chem. Soc., Chem. Comm.* **1994**, (8), 947.
- (5) Xu, Q.; Inoue, S.; Tsumori, N.; Mori, H.; Kameda, M.; Tanaka, M.; Fujiwara, M.; Souma, Y. *J. Mol. Catal. A: Chem.* **2001**, *170* (1–2), 147.
- (6) Stepanov, A. G.; Luzgin, M. V.; Romannikov, V. N.; Sidelnikov, V. N.; Zamaraev, K. I. *J. Catal.* **1996**, *164* (2), 411.
- (7) Cheung, P.; Bhan, A.; Sunley, G. J.; Iglesia, E. *Angew. Chem., Int. Ed.* **2006**, *45* (10), 1617.
- (8) Cheung, P.; Bhan, A.; Sunley, G. J.; Law, D. J.; Iglesia, E. *J. Catal.* **2007**, *245* (1), 110.

adsorbed upon contact with ambient air and to convert exchanged NH_4^+ cations to H^+ . $\text{NH}_4\text{-MOR}$ ($\text{Si}/\text{Al} = 10$, Zeolyst, ~ 14 g) was partially exchanged with Na^+ using 0.5 L of aqueous NaNO_3 solutions (99%, EMD Chemicals, 0.014–2.44 M) at 353 K for 12 h and then washed in 2 L of deionized water and isolated by filtration. The resulting solids were treated at 393 K overnight in ambient air and then for 3 h at 773 K (0.0167 K s^{-1}) in flowing dry air (zero grade, Praxair). $\text{NH}_4\text{-MOR}$ ($\text{Si}/\text{Al} = 10$, Zeolyst, ~ 2.5 g) was exchanged with Co^{2+} cations using 0.1 L of aqueous $\text{Co}(\text{NO}_3)_2 \cdot 6\text{H}_2\text{O}$ (98+%, Sigma-Aldrich, CAS 10226-22-9, 0.1 M) solutions at 353 K for 24 h and then washed in 0.5 L of deionized water and isolated by filtration. The resulting solids were dried at ambient temperatures overnight and then treated in flowing dry air (zero grade, Praxair) for 3 h at 773 K (0.0167 K s^{-1}). Na and Co contents were measured by inductively coupled plasma optical emission spectroscopy (ICP-OES) (Galbraith Laboratories); the fraction of ion exchange for these samples is reported in Figure 2.

Catalytic Carbonylation of Dimethyl Ether. Steady-state DME carbonylation rates and selectivities were measured in a packed-bed reactor (8.1 mm i.d.; 9.5 mm o.d.) equipped with a thermocouple held within a concentric thermowell (1.6 mm) aligned along the tube center. Catalyst samples (0.5 g, 125–250 μm aggregates) were treated in flowing dry air for 3 h at 773 K (0.0167 K s^{-1}) and cooled to reaction temperature (438 K) in flowing He ($1.67 \text{ cm}^3 \text{ s}^{-1}$) before reaction with premixed reactant mixtures (2% DME/93% $\text{CO}/5\%$ Ar; $1.67 \text{ cm}^3 \text{ s}^{-1}$); reactants were dried before use by flowing through a CaH_2 bed (0.5 g, 99.99%, Aldrich) held at ambient temperature. Heat-traced lines (423–473 K) were used to transfer the reactor effluent into a mass spectrometer (MKS Spectra Minilab; 1–90 amu) and a gas chromatograph (Agilent 6890) equipped with a methyl siloxane capillary column (HP-1, 50 m \times 0.32 mm \times 1.05 μm) connected to a flame ionization detector and a Porapak Q packed column (80–100 mesh, 12 ft \times 1/8 in) connected to a thermal conductivity detector. Pyridine (Sigma-Aldrich, 99.9%, CAS 110-88-1) was introduced into DME/ CO/Ar reactant streams (2/93/5; $1.5 \text{ cm}^3 \text{ s}^{-1}$) using a saturator maintained at 273 K using a He flow ($0.17 \text{ cm}^3 \text{ s}^{-1}$) to titrate Brønsted acid sites and to determine their concentration and their role in DME carbonylation reactions.

Infrared Spectroscopic Studies of Proton-Exchanged and Cation-Exchanged Zeolites. Infrared spectra were measured in the 4000–400 cm^{-1} region on self-supporting wafers (~ 20 –40 mg) held within a quartz vacuum cell with NaCl windows. Spectra were acquired using a Nicolet NEXUS 670 infrared spectrometer equipped with a Hg–Cd–Te (MCT) detector. Each spectrum was obtained by averaging 64 scans collected at 2 cm^{-1} resolution. Samples were treated in flowing dry air ($\sim 1.67 \text{ cm}^3 \text{ s}^{-1}$, zero grade, Praxair) at 723 K for 2 h, evacuated at 723 K for 2 h using a diffusion pump (<0.01 Pa dynamic vacuum; Edwards E02), and cooled to ambient temperatures (~ 303 K) in a vacuum before measuring spectra.

Infrared Spectroscopic Studies of Propane, *n*-Hexane, Pyridine, and 2,6-Dimethyl Pyridine Probe Molecules. *n*-Hexane (Sigma-Aldrich, $\geq 99\%$), pyridine (Sigma-Aldrich, $\geq 99.9\%$), and 2,6-dimethyl pyridine (Sigma-Aldrich, 99+%) were dosed onto H-MOR ($\text{Si}/\text{Al} = 10$, Zeolyst) at ambient temperatures (~ 303 K) to measure the number of H^+ in 8-MR and 12-MR channels. *n*-Hexane, pyridine, and 2,6-dimethyl pyridine were purified by multiple freeze–thaw cycles before dosing from the vapor phase. Sample treatment protocols were identical to those described above. The pressure of the probe molecules was increased stepwise by dosing from a control volume; infrared spectra were collected 180s after each dose without intervening evacuation. Pressures were measured with a MKS BARATRON pressure transducer (type 127). *n*-Hexane and propane (Praxair, 20%; balance He) were also dosed onto H-FER ($\text{Si}/\text{Al} = 33.5$, Zeolyst) at ambient temperatures (~ 303 K) to determine the concentration of H^+ in 8-MR and 10-MR channels of FER.

Results and Discussion

Distribution of H^+ Sites in MOR and FER. H-MOR consists of 12-MR main channels with intersecting 8-MR channels (side pockets). Al substitution into the neutral silicate framework creates a charge imbalance compensated by cations (e.g., O–H group that act as Brønsted acids). The shift in frequency for the antisymmetric O–H stretch in H-MOR during adsorption of probe molecules of varying size has been used to detect two types of O–H species, with bands at $\sim 3610 \text{ cm}^{-1}$ for H^+ in 12-MR channels and at $\sim 3590 \text{ cm}^{-1}$ for H^+ sites in 8-MR side pockets.^{9–11} We have used singular value decomposition (SVD) and spectral analysis methods reported by Garland et al.^{12–14} to determine band positions and relative concentrations of O–H groups in 8-MR and 12-MR channels of MOR (sections 1.1–1.3; Supporting Information). The fraction of H^+ sites within 8-MR and 12-MR channels in H-MOR was determined to be 0.55 and 0.45 (± 0.05), respectively, for this sample.

Eder and Lercher^{15–17} have shown that alkane adsorption is localized on Brønsted acid sites within zeolite channels via hydrogen bonding between alkanes and Si–OH–Al groups at temperatures below 373 K. *n*-Hexane adsorption on H-MOR led to an asymmetric O–H band with maxima centered at 3590 and 3610 cm^{-1} ; the intensity of this band decreased to only 0.67 of its initial value as the *n*- C_6H_{14} pressure increased to 10 mbar and the band shifted to lower frequencies, indicating that *n*-hexane perturbs only O–H groups within 12-MR channels. The inability of *n*-hexane to interact with H^+ sites in 8-MR channels of FER was also reported by van Well et al.^{18,19} Figure 1 shows the O–H region infrared spectra for H-MOR ($\text{Si}/\text{Al} = 10$, Zeolyst) after exposure to *n*-hexane at 303 K. A broad band typical of hydrogen-bonded (perturbed) OH groups appeared at lower wavenumbers upon hexane dosing. The pronounced asymmetry of the perturbed hydroxyl groups confirmed that *n*-hexane molecules did not interact with OH groups within 8-MR channels. Band deconvolution analysis of infrared spectra measured at increasing *n*-hexane pressures (shown in the inset of Figure 1) showed that 55–60% of the H^+ sites are located in the 8-MR channels and that *n*-hexane perturbs only H^+ sites within 12-MR channels.

The selective titration of OH groups within 12-MR channels of MOR by pyridine¹⁰ and alkyipyridines²⁰ has also been reported. We have also dosed pyridine and 2,6-dimethylpyridine

- (9) Datka, J.; Gil, B.; Kubacka, A. *Zeolites* **1997**, *18* (4), 245.
- (10) Maache, M.; Janin, A.; Lavalley, J. C.; Benazzi, E. *Zeolites* **1995**, *15* (6), 507.
- (11) Makarova, M. A.; Wilson, A. E.; van Liemt, B. J.; Mesters, C.; de Winter, A. W.; Williams, C. J. *Catal.* **1997**, *172* (1), 170.
- (12) Gao, F.; Allian, A. D.; Zhang, H. J.; Cheng, S. Y.; Garland, M. *J. Catal.* **2006**, *241* (1), 189.
- (13) Allian, A. D.; Tjahjono, M.; Garland, M. *Organometallics* **2006**, *25* (9), 2182.
- (14) Chen, L.; Garland, M. *Appl. Spectrosc.* **2003**, *57* (3), 331.
- (15) Eder, F.; Stockenhuber, M.; Lercher, J. A. Sorption of light alkanes on H-ZSM5 and H-Mordenite. *Zeolites: A Refined Tool For Designing Catalytic Sites*; Elsevier Science: 1995; Vol. 97, pp 495.
- (16) Eder, F.; Lercher, J. A. *J. Phys. Chem. B* **1997**, *101* (8), 1273.
- (17) Eder, F.; Stockenhuber, M.; Lercher, J. A. *J. Phys. Chem. B* **1997**, *101*, 5414.
- (18) van Well, W. J. M.; Cottin, X.; de Haan, J. W.; Smit, B.; Nivarthi, G.; Lercher, J. A.; van Hooff, J. H. C.; van Santen, R. A. *J. Phys. Chem. B* **1998**, *102* (20), 3945.
- (19) van Well, W. J. M.; Cottin, X.; Smit, B.; van Hooff, J. H. C.; van Santen, R. A. *J. Phys. Chem. B* **1998**, *102* (20), 3952.
- (20) Nesterenko, N. S.; Thibault-Starzyk, F.; Montouillout, V.; Yuschenko, V. V.; Fernandez, C.; Gilson, J.-P.; Fajula, F.; Ivanova, I. I. *Microporous Mesoporous Mater.* **2004**, *71* (1–3), 157.

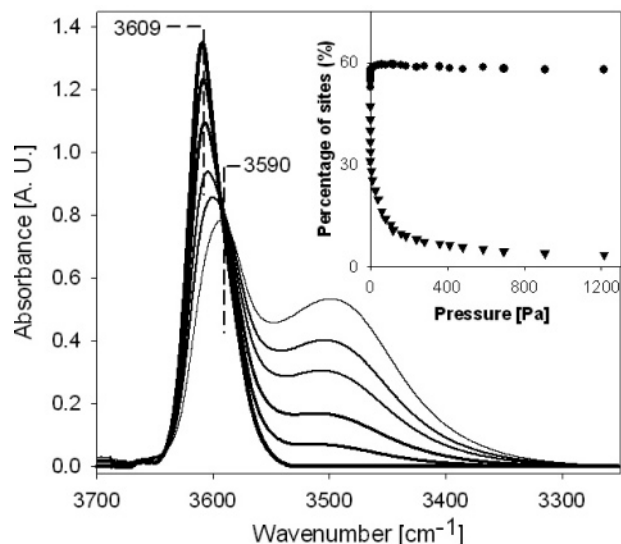


Figure 1. Infrared spectra of the OH stretching region of HMOR (Si/Al = 10, Zeolyst) upon *n*-hexane adsorption at 303 K. Inset shows the percentage of H⁺ sites determined from band deconvolution analysis in 8-MR (●) and 12-MR (▼) channels with increasing *n*-hexane pressure.

on H-MOR to determine the concentration of H⁺ in 8-MR and 12-MR channels. Contact with pyridine led to bands at 1545 cm⁻¹, assigned to pyridine on Brønsted sites (B), and at 1491 cm⁻¹, assigned to pyridine on Brønsted and Lewis sites (B + L). Band deconvolution of infrared spectra recorded at increasing pyridine and 2,6-dimethyl pyridine pressures showed that these strong bases titrate all H⁺ sites within 12-MR channels in MOR, but they perturb only a small fraction (<15%) of the OH groups within 8-MR channels, possibly those located near the intersections of 8-MR and 12-MR channels. The fraction of the initial OH groups perturbed by these molecules is consistent with the number of OH groups in 12-MR channels measured by spectral deconvolution of the O–H bands without adsorbed molecules and from perturbation of O–H bands upon adsorption of *n*-hexane (Figure S4; Supporting Information). These independent measurements confirmed that 0.55 (±0.05) of the OH groups in this H-MOR sample (Si/Al = 10, Zeolyst) reside within 8-MR channels.

n-Hexane adsorption on H-FER (Si/Al = 33.5, Zeolyst) perturbed >85% of the OH groups, as also reported by van Well et al.,^{18,19} who also concluded, based on ¹³C CP MAS NMR studies, that *n*-hexane adsorption on H-FER was similar to that on NaZSM-22, (structural code TON; 10-MR one-dimensional channel system) and that *n*-hexane adsorbed only on sites located within 10-MR channels of H-FER. This conclusion was confirmed by configurational bias Monte Carlo simulations, in which *n*-hexane was found to adsorb only within 10-ring channels in FER even at high pressures (6.3 MPa). In contrast, propane interacts preferentially with OH groups within 8-MR channels of FER, because of stronger dispersive interactions within smaller 8-MR channels compared to 10-MR channels. Singular value decomposition (SVD) analysis of the OH region infrared spectra at different propane pressures was used to deconvolute O–H bands within 8-MR (~3590 cm⁻¹) and 10-MR (~3600 cm⁻¹) channels in H-FER. These deconvolution methods for spectra measured in the presence of propane or *n*-hexane showed that the fraction of the OH groups within 8-MR channels in H-FER (Si/Al = 33.5, Zeolyst) was 0.11 (±0.04).

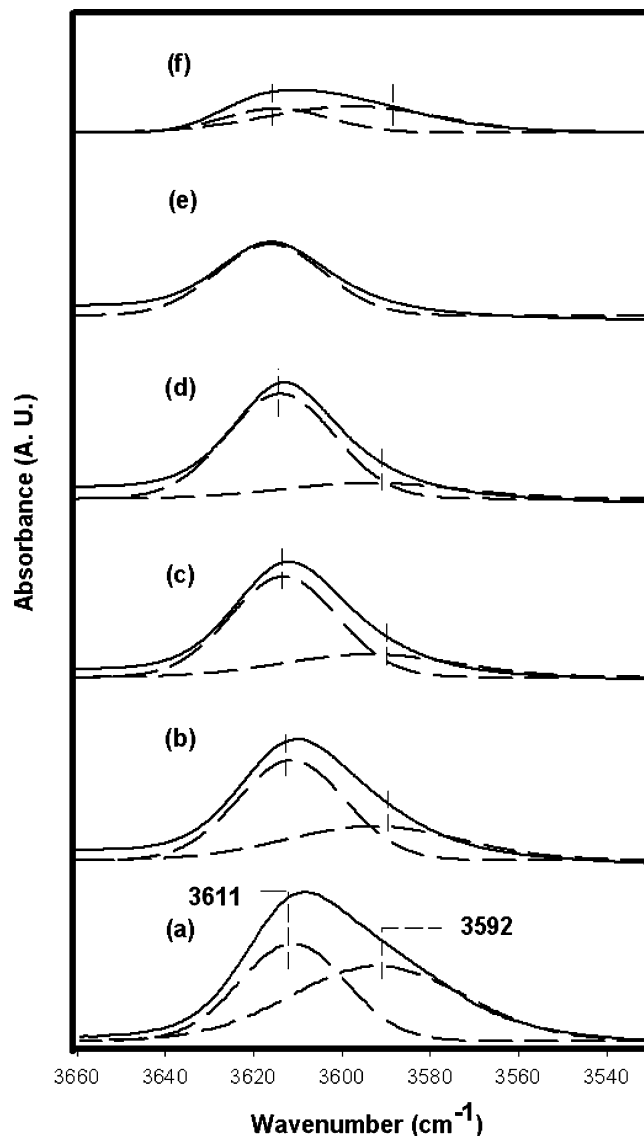


Figure 2. Infrared spectra (—) and deconvoluted bands corresponding to H⁺ in 8-MR and 12-MR channels (---) of (a) H₁₀₀Na₀MOR, (b) H₈₃Na₁₇-MOR, (c) H₇₃Na₂₇MOR, (d) H₅₉Na₄₁MOR, (e) H₄₅Na₅₅MOR, and (f) H₂₉Co₃₂MOR.

Distribution of H⁺ Sites in Cation-Exchanged MOR Samples.

Figure 2 shows the infrared spectra in the OH stretching region for H-MOR, as Na⁺ and Co²⁺ replaced some of the H⁺ species, a process that significantly decreased DME carbonylation turnover rates (per total H⁺).⁸ The OH bands in MOR became more symmetrical with increasing Na⁺ content, because of a preferential weakening of the band corresponding to OH groups within 8-MR (at 3592 cm⁻¹) as Na⁺ replaced H⁺; these data indicate that Na exchange occurred selectively by replacement of H⁺ within 8-MR side pockets. The selective replacement of H⁺ in side pockets of MOR by Na⁺ was previously reported.^{10,21} Co²⁺, in contrast to Na⁺, replaced H⁺ with similar probability in 8-MR and 12-MR channels. Taken together with the sharp decrease in carbonylation rates (per total H⁺) upon Na exchange (Figure 3), these data implicate a specific reactivity of CH₃ intermediates within 8-MR channels in carbonylation steps. The number of H⁺ sites within 8-MR

(21) Veeffkind, V. A.; Smidt, M. L.; Lercher, J. A. *Appl. Catal. A: General* **2000**, *194*, 319.

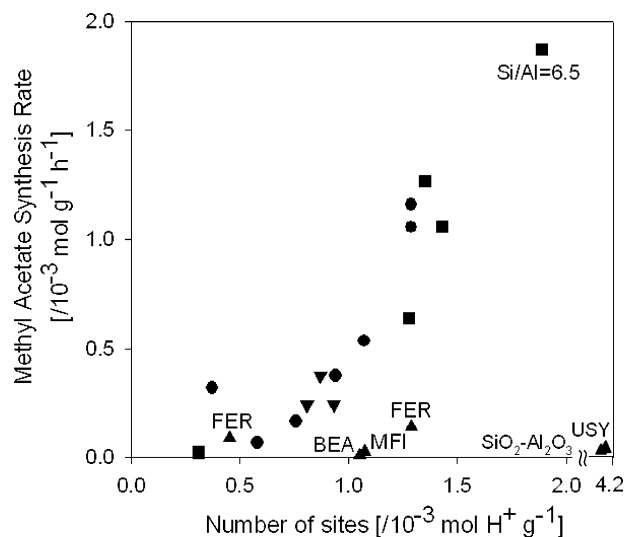


Figure 3. DME carbonylation rates (438 K, $3.34 \text{ cm}^3 \text{ s}^{-1} \text{ g}^{-1}$, 0.93 MPa CO, 20 kPa DME, 50 kPa Ar) plotted against the number of total H^+ sites in (i) H-MOR (Si/Al = 10, Zeolyst) and cation-exchanged MOR samples reported in Figure 2 (●); (ii) H-MOR samples with Si/Al = 6.5 and Si/Al ~ 10 (■); (iii) H-MFI (Si/Al = 12.2), H-BEA (Si/Al = 12.5), H-USY (Si/Al = 3), amorphous silica–alumina (Si/Al = 3), and H-FER (Si/Al = 10 and 33.5) (▲); and (iv) H-MOR (Si/Al = 10, Zeolyst) after chemical dealumination by oxalic acid treatments with Si/Al ratios of 14–17 (▼). Details regarding synthesis and treatment protocols for (ii), (iii), and (iv) were reported in refs 7 and 8.

channels decreased upon exchange by a factor of ~ 10 when only 0.55 of the (total) H^+ species were replaced by Na^+ in H-MOR. In contrast, the fraction of H^+ species within 12-MR channels was essentially unchanged by Na^+ exchange (0.45 ± 0.05) when 0.55 of the total H^+ were replaced by Na^+ .

Correlation between DME Carbonylation Rates and the Number of OH Groups. Figure 4 shows DME carbonylation rates (per g) as a function of the number of OH groups (per g) located within 8-MR (MOR, FER) or 12-MR (MOR) channels for samples with varying Na or Co content. Carbonylation rates increased in parallel with the number of H^+ sites within 8-MR channels. In contrast, no correlation with the number of H^+ sites within 12-MR (MOR) channels or with the total number of H^+ sites is evident from these data (Figure 4, inset). Such specificity in the reactivity for O–H sites of identical composition when placed within a more restrictive environment appears to be unprecedented for inorganic systems. Veeffkind et al.²¹ reported that rates of ethanol reactions with NH_3 are ~ 1.5 times higher on H^+ sites within 8-MR pockets in H-MOR than on H^+ sites within 12-MR channels; these authors proposed that monoethyl amine intermediates were selectively stabilized within 8-MR channels. We find here that CH_3 intermediates confined within 8-MR channels react with CO much more rapidly than similar species within 10-MR (FER) or 12-MR (MOR) channels, apparently because of specific stabilization of the acetyl-like transition states or of CO molecules as they approach CH_3 groups when such events occur within more constrained spatial geometries. The unique reactivity of H^+ (and CH_3) within 8-MR channels is consistent with the high DME carbonylation rates on H-MOR and H-FER, which contain 8-MR channels and with the much lower and often undetectable reactivity of OH (CH_3) sites with similar local composition in H-MFI and H-BEA zeolites and in H-USY and amorphous silica–alumina samples with higher Al content (Si/Al = 3) (Figure 3).⁷ These findings

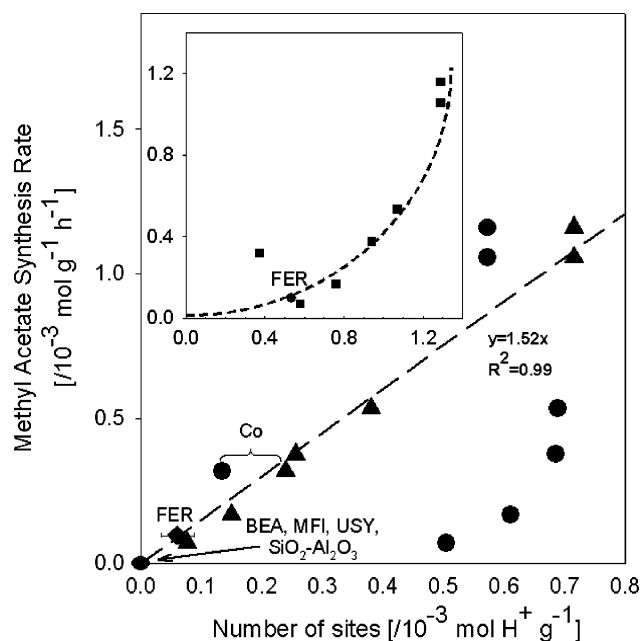


Figure 4. DME carbonylation rates per unit mass (438 K, $3.34 \text{ cm}^3 \text{ s}^{-1} \text{ g}^{-1}$, 0.93 MPa CO, 20 kPa DME, 50 kPa Ar) plotted against the number of H^+ sites per unit mass in 8-MR channels of MOR (▲; Si/Al = 10, Zeolyst) and FER (◆; Si/Al = 33.5, Zeolyst) and 12-MR channels of MOR (●). Inset shows DME carbonylation rates plotted against the total number of H^+ sites in these samples (■).

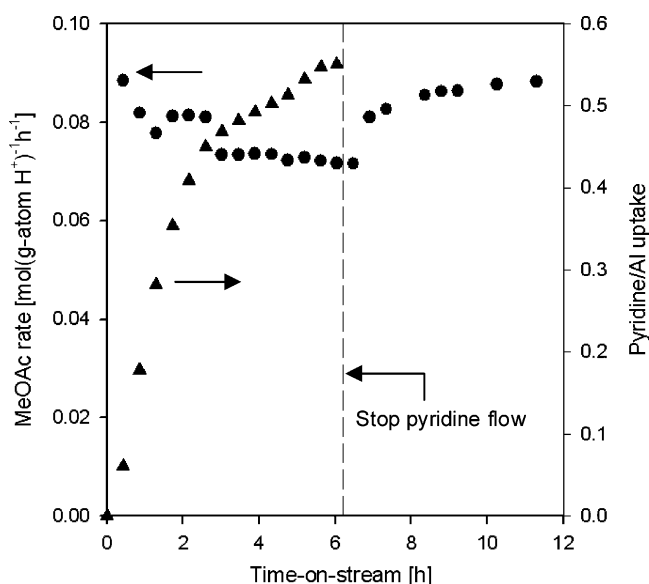


Figure 5. DME carbonylation rates (●; per total H^+) and pyridine uptake (▲; Pyridine/Al) plotted against the time-on-stream (h) during pyridine titration experiments on HMOR (Si/Al = 10, Zeolyst; 423 K, 1 atm of total pressure).

and conclusions are also consistent with the marked differences in turnover rates (per total H^+) for H-MOR with nominally similar Si/Al ratios but different origin (Figure 3) and with the lower turnover rates (per total H^+) in dealuminated MOR samples with high Si/Al ratios; dealumination led to the preferential loss of accessible Al sites within 8-MR channels, either by removing them or by making such channels less accessible.⁸

Figure 5 shows DME carbonylation rates (per total H^+) for HMOR (423 K; 1 bar total pressure) upon pyridine addition to DME/CO/Ar reactant mixtures. DME carbonylation rates de-

creased by less than 15% even after adsorption of 0.5 pyridine molecules per OH group. These data indicate that either pyridine did not interact strongly with CH₃ species prevalent during steady-state DME carbonylation or the reactivity of H⁺ (CH₃) in 8-MR channels, inaccessible to pyridine because of steric constraints, contributed most of the active sites relevant to steady-state DME carbonylation catalysis; the reactivity of H⁺ (CH₃) in 12-MR channels, which are readily titrated by pyridine, must be therefore significantly lower than that of species of similar composition located within 8-MR channels.

The fractional change in the intensity of the OH infrared bands upon exposure to pyridine was very similar ($\pm 10\%$) to the number of pyridine molecules adsorbed per Al site during DME carbonylation. These data indicate that extinction coefficients for OH groups located in 8-MR and 12-MR channels are similar. Makarova et al.¹¹ reported that OH groups in 8-MR channels have a slightly higher extinction coefficient ($3.8 \mu\text{mol g}^{-1}$) than that for OH groups in 12-MR channels ($2.5 \mu\text{mol g}^{-1}$). Our deconvolution procedures differ from those in the previous study; we use only one primary component to describe the high-frequency and low-frequency OH bands (compared to three primary components used by Makarova et al.¹¹) and allow the peak shape to be optimized instead of choosing arbitrary shapes (65% Lorentzian and 35% Gaussian used by Makarova et al.¹¹). Thus, we have not used these previously reported extinction coefficients. We note that a difference in extinction coefficients of 1.5 between these two bands changes only the slope and not the linearity of the correlation between carbonylation rates and the number of H⁺ sites in 8-MR channels (Figure 4).

Implications for Carbonylation Catalysis. Zecchina et al.^{22,23} used infrared spectroscopy to probe neutral and hydrogen-bonded complexes formed by interactions of H₂O with acidic OH groups in H-MFI, H-MOR, and H-Nafion. Bands for [H(H₂O)_{*n*}]⁺ ionic species (at 1860–1650 cm⁻¹ and 1450 cm⁻¹) appeared in H-MOR even at the lowest H₂O pressures, indicating that OH groups within narrow 8-MR channels in MOR stabilize ionic clusters more effectively than within larger channels in H-MFI. Hence, it appears plausible that the strong water inhibition of DME (and methanol) carbonylation^{7,8} reflects the selective formation of unreactive [(CH₃)(H₂O)_{*n*}]⁺ cationic clusters within 8-MR channels, where CO insertion into CH₃ groups selectively occurs. Haw et al.²⁴ have proposed that high dielectric constant solvents favor proton transfer in zeolites by stabilizing ion-pair structures. Similarly, 8-MR channels that selectively stabilize ionic H₂O clusters may also provide a more polar environment, which is likely to favor ionic transition states involved in CO insertion into bound methyl groups.

Clark et al.²⁵ have described the dearth of firm evidence for transition state selectivity, wherein the *local* shape of the zeolite pore influences *local* reactions to form a given product by selective stabilization of the required transition state *without* detectable effects on bound reactants (CH₃) or products (CH₃-CO). Previous ¹³C MAS NMR studies did not detect any spectral differences among CH₃ groups within various zeolite structures

(chemical shifts of 59.9 ppm on H-MFI, 60.7 ppm on HMOR, 49 ppm on H-ZSM-11, 56 ppm on H-FAU),^{26–28} in sharp contrast with the marked reactivity differences that we report here for their reactions with CO. Zeolites (H-MFI, H-MOR, H-FER) with markedly different carbonylation turnover rates chemisorbed DME with a saturation stoichiometry of 0.5 (± 0.05) DME/Al at 423 K;^{7,8} thus, all OH groups, irrespective of their spatial environment, form saturation coverages of CH₃ groups at conditions of carbonylation catalysis. Hence, we propose here that DME carbonylation on acidic zeolites and its rate-determining elementary step (insertion of CO into CH₃ groups) represent an example of transition state selectivity in which charged transition states are stabilized to a much greater extent than adsorbed (neutral) CH₃ reactants and CH₃CO products. The charged transition state benefits from concerted interactions with lattice oxygens within the smaller 8-MR channels. These interactions become weaker within larger 10-MR and 12-MR channels. In contrast, neutral reactants and products are stabilized by local covalent bonds with framework oxygen atoms vicinal to Al sites. These bonds are only weakly affected by more distant oxygen atoms, the precise location of which varies with zeolite structure and specifically with their presence within 8-MR, 10-MR, and 12-MR channels. We consider these effects of confinement on the transition state for carbonylation of methyls to acetyls to differ in concept and detail from size exclusion effects denoted in previous studies as “restricted transition state shape selectivity”²⁹ and also from the “active site shape selectivity” described by Anderson and Klinowski³⁰ in which the zeolite structure determines the relative abundance of adsorbed intermediates by steric restrictions on isomerization pathways. The specificity of 8-MR channels for CH₃*-CO reactions reported here represents an unprecedented example of molecular reactivity controlled by confinement within microporous solids with conceptual analogues in enzyme catalysis.³¹

The evidence presented indicates a direct correspondence between DME carbonylation rates and the number of H⁺ sites present within 8-MR channels in MOR and FER. In light of this, improved catalysts will require zeolite frameworks in which (i) 8-MR channels and pockets can be accessed from external crystal surfaces via larger interconnected channels and (ii) H⁺ (and framework Al atoms) can be selectively placed within such 8-MR channels and pockets. The data presented provide a compelling experimental demonstration of transition state selectivity and a unique opportunity to design microporous structures to match the stringent spatial constraints required to stabilize specific transition states in catalytic reactions.

Acknowledgment. The authors dedicate this article to the memory of Dr. John P. Collins. His leadership within the BP technical staff was instrumental in the birth and growth of the Methane Conversion Cooperative program that led to the findings reported herein. The authors acknowledge financial support from BP as part of the Methane Conversion Coop-

- (22) Zecchina, A.; Geobaldo, F.; Spoto, G.; Bordiga, S.; Ricchiardi, G.; Buzzoni, R.; Petrini, G. *J. Phys. Chem.* **1996**, *100* (41), 16584.
(23) Zecchina, A.; Spoto, G.; Bordiga, S. *Phys. Chem. Chem. Phys.* **2005**, *7* (8), 1627.
(24) Haw, J. F.; Xu, T.; Nicholas, J. B.; Goguen, P. W. *Nature* **1997**, *389* (6653), 832.
(25) Clark, L. A.; Sierka, M.; Sauer, J. *J. Am. Chem. Soc.* **2004**, *126* (3), 936.

- (26) Derouane, E. G.; Gilson, J. P.; Nagy, J. B. *Zeolites* **1982**, *2* (1), 42.
(27) Ivanova, I. I.; Corma, A. *J. Phys. Chem. B* **1997**, *101* (4), 547.
(28) Jiang, Y. J.; Hunger, M.; Wang, W. *J. Am. Chem. Soc.* **2006**, *128* (35), 11679.
(29) Csicsery, S. M. *Zeolites* **1984**, *4* (3), 202.
(30) Anderson, M. W.; Klinowski, J. *J. Am. Chem. Soc.* **1990**, *112* (1), 10.
(31) Mesecar, A. D.; Stoddard, B. L.; Koshland, D. E. *Science* **1997**, *277* (5323), 202.

erative Research Program and helpful technical discussions with Dr. Patricia Cheung (University of California at Berkeley), Professor Avelino Corma (Universidad Politecnica de Valencia), and Professor Johannes Lercher (Technical University of Munich).

Supporting Information Available: Band deconvolution methods used. This material is available free of charge via the Internet at <http://pubs.acs.org>.

JA070094D